25th ABCM International Congress of Mechanical Engineering
October 20-25, 2019, Uberlândia, MG, Brazil

COBEM-2019-0694
AN ANALYTICAL-BASED OPTIMIZATION APPROACH TO PRELIMINARY WEIGHT SIZING OF AIRCRAFT WINGS

Alexandre Acerra Gil
Thiago Augusto Machado Guimarães
Federal University of Uberlândia, School of Mechanical Engineering, Uberlândia, MG, 38400-902, Brazil
alexandre.gil@ufu.br, thiagoamg@ufu.br

Abstract. *This work presents the development of an analytical-based optimization approach capable of performing a preliminary weight sizing of aircraft wings during the conceptual or preliminary design phases. Analytical methods were used in order to generate a faster calculation logic when compared with numerical simulations adopted during more advanced design phases. Aerodynamic formulations allowed the estimation of the lift coefficient and its transformation into a two-dimensional spanwise load distribution. As the wing box structure is highly complex for the application of analytic equations, simplifications had to be applied to idealize the structure. With the loads and the idealized structure, the normal stresses and shear flow could be calculated. Design criteria were then applied to verify if the structure would be able to withstand the applied loads. Finally, this calculation routine was introduced in an optimization algorithm to find the lowest possible weight wing configuration, creating the basis of a sizing tool. The validation was performed by comparing the sizing responses with numerical simulations using the finite element method.*

Keywords: *aeronautical design, structure optimization, preliminary weight sizing, aircraft wing, analytical method*

1. INTRODUCTION

The study of techniques for aeronautical design has been a subject of discussion among engineers in the industry for a long time. With an increasingly competitive market, more efficient and accurate methods motivate the development of new methods for preliminary sizing.

Until the mid-1950s, the industry was widely based on statistical methodologies for the development of its projects (Torenbeek, 2013). Although it is an approximation that can be performed with virtually no calculation cost, its accuracy margin can be quite questionable, especially if it is related to innovative designs, without a concrete historical database.

With the advent of the Cold War, new computational techniques such as finite element method and computational fluid dynamic were created. These new technologies caused a revolution in the way aircraft were designed, where projects of that era are considered revolutionary even today (Murman and Rizzi, 2002). Conversely, these methods could be very complex to apply on preliminary design phases due to its high computational cost.

Consequently, numerous studies have been developed in order to maximize the performance of sizing tools. A great solution found is based on the use of multidisciplinary optimization (MDO). This methodology explores the design process incorporating interactions between different project disciplines (e.g., structures, aerodynamics, stability and performance). Besides, MDO can consider uncertainties and nonlinear situations, becoming a highly reliable resource (McMasters and Cummings, 2002).

A technical study based on papers presented at the European-U.S. Multi-Disciplinary Optimization Colloquium over the last years presented a perspective that MDOs are increasingly using analytical methods instead of computational simulations (de Weck *et al.*, 2007). The main cause of this trend is that analytical approaches are able to perform design calculations very rapidly, making the optimization process more efficient.

Along those lines, this work presents an analytical-based optimization approach that allows the design and weight estimation of aircraft wings, which can also be incorporated into a multi-disciplinary optimization process.

2. METHODS

2.1 Aerodynamic Loads

Aerodynamic loads acting on the wing are estimated through empirical methods proposed in the literature. The lift coefficient estimation for a swept finite three-dimensional wing is based on the "linearized small-perturbation potential method". Equation 1 presents the formulation that allows the global subsonic lift coefficient $C_{L_{M\leq 1}}$ calculation proposed

by Bonnet and Luneau (1989).

$$C_{L_{M\leq 1}} = \frac{\pi AR}{1+\sqrt{1+\left(\frac{AR}{2\cos\Lambda}\right)^2\left(1-(M_\infty\cos\Lambda)^2\right)}} \tag{1}$$

where M_∞ is the Mach number, AR is the aspect ratio, and Λ is the sweep angle of the wing.

With the wing geometry and the lift coefficient value, it is possible to calculate a two-dimensional lift distribution along the wingspan through a semi-empirical method known as the "Schrenk approximation" (Schrenk, 1941). This approximation proposes that the variation of the chord along the wingspan is the arithmetic mean between the studied wing and a hypothetical elliptic wing of same span and area. As has been noted, this estimation is a two-dimensional distribution, as a result, its position along the chord is defined at the wing's center of pressure, i.e. it is a line that represents a resultant force of the pressure field acting on the three-dimensional wing. Equation 2 shows the lift distribution along the wingspan.

$$w(y) = qS_{\text{wing}}\frac{(1+\lambda)\,2b\sqrt{1-\left(\frac{2y}{b}\right)^2}+\pi b\left[1+\left(\frac{2y}{b}\right)(\lambda-1)\right]}{(1+\lambda)\,\pi b^2}C_{L_{\text{wing}}}^2 n \tag{2}$$

where S_{wing}, b, and λ represent respectively the area, span, and taper ratio of the wing, $C_{L\,\text{wing}}$ represents the lift coefficient calculated by Eq. (1), q represents the dynamic pressure, y represents the position along the wingspan, and n represents the load factor.

Consequently, the shear stress $S(y)$ and the bending moment $M(y)$ distributions along the wingspan can be calculated by Eqs. (3) and (4), respectively.

$$S(y) = \int_0^{b/2} w(y)\,dy = \sum_{i=1}^{n-1}\left(\frac{w_i+w_{i+1}}{2}\right)\Delta y \tag{3}$$

$$M(y) = \int_0^{b/2} S(y)\,dy = \iint_0^{b/2} w(y)\,dy = \sum_{i=1}^{n-1}\left(\frac{S_i+S_{i+1}}{2}\right)\Delta y \tag{4}$$

where $w(y)$ is the lift distribution along the wingspan calculated by Eq. (2) and Δy is the span increment, varying according to the discretization chosen for the calculation.

2.2 Structural Idealization

In order to analyze a complex structure, in this case, a wing box structure, simplifications had to be made to facilitate the sizing process. The wing structure can be idealized into a simpler mechanical model, which has mechanical properties equivalent to the real structure.

Therefore, the structural idealization method proposed by Megson (2016) is used to replace the wing structural elements by concentrated zones known as booms.

As a result, a skin panel with a finite thickness is idealized as an infinitesimal thin plate with two finite booms in each row. Figure 1 shows how the idealization of a panel is made.

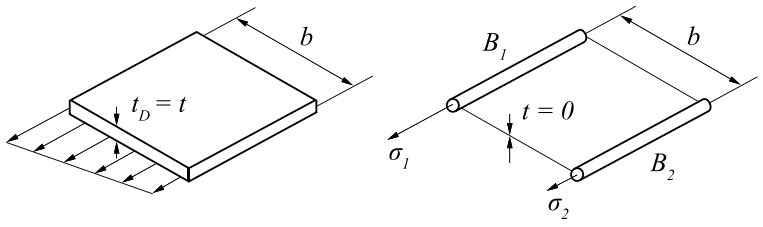

(a) Real panel (b) Idealized panel

Figure 1. Panel Idealization. (Megson, 2016)

Since the normal forces in the real and idealized panels must be the same, the Eq. (5) of balance of forces is used for the boom 1.

$$\sigma_2 t_D\frac{b^2}{2}+\frac{1}{3}(\sigma_1-\sigma_2)\,t_D b^2 = \sigma_1 B_1 \tag{5}$$

where t_D is the thickness of the real panel, b is the panel length, and σ_1 and σ_2 are the normal stresses on booms 1 and 2, respectively.

On the other hand, the values of σ_1 and σ_2 are not known, so Megson (2016) assumes their values as the vertical distance between the boom and the section's centroid, i.e. the factors σ_1 and σ_2 are approximated by the heights of the boom in the wing section as z_1 and z_2.

With the rearrangement of Eq. (5), the boom 1 area can be calculated by Eq. (6).

$$B_1 = \frac{t_D b}{6}\left(2 + \frac{z_2}{z_1}\right) \tag{6}$$

Similarly, the boom 2 area can be calculated by Eq. (7).

$$B_2 = \frac{t_D b}{6}\left(2 + \frac{z_1}{z_2}\right) \tag{7}$$

Moreover, the booms positions depend on considerations adopted by the designer. Rivello (1969) suggests positioning them at the central portion of each skin panel and the joint point between spars and skin panels. In this way, the spars will withstand most of normal stresses, while the skin panels will withstand most of shear stresses. In the case that there is a stiffener positioned between two booms, its cross-sectional area is added to the equations. Figure 2 shows the method proposed in the literature.

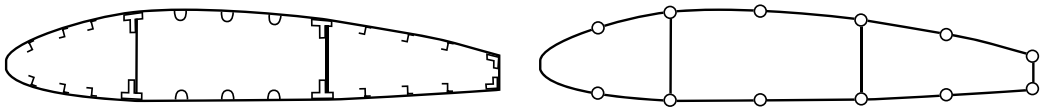

(a) Real wing cross-section (b) Idealized wing cross-section

Figure 2. Wing cross-section idealization. (Rivello, 1969)

2.3 Normal Stress

After the structure idealization was performed, the previously unknown normal stresses acting on the booms can be calculated using the shear force and bending moment distributions. Equation 8 shows the normal stress calculation in a boom i.

$$\sigma_{y_i} = -\left(\frac{M_z I_{xx} + M_x I_{xz}}{I_{xx} I_{zz} - {I_{xz}}^2}\right) x_i + \left(\frac{M_x I_{zz} + M_z I_{xz}}{I_{xx} I_{zz} - {I_{xz}}^2}\right) z_i \tag{8}$$

where x_i and z_i are the boom i coordinates in relation to the section's centroid, M_x and M_z are the bending moments in the x and z directions, respectively, and I_{xx}, I_{zz} and I_{xz} are the moment of inertia in the x, z, and xz directions of the idealized section, respectively. In this study, only the forces generated by the lift were estimated, therefore only M_z values are considered.

Conversely, in most wing projects, the sections along the wingspan are not constant due to the effect of variable geometry (torsion, swept angle, and taper ratio). This geometry variation also generates stresses in the x and z direction, which must be taken into account. The components σ_x and σ_z are calculated using Eqs. (9) and (10), respectively.

$$\sigma_{xi} = \sigma_{y_i}\frac{\delta x_i}{\delta y_i} \tag{9}$$

$$\sigma_{zi} = \sigma_{y_i}\frac{\delta z_i}{\delta y_i} \tag{10}$$

where δx_i and δz_i are the variation of the position of a boom i along a span variation δy_i in the x and z directions, respectively.

2.4 Shear Flow

The shear flow calculation is performed in three steps. Firstly, a pure shear flow is calculated using the shear stresses previously estimated by the aerodynamics calculations. Next, a shear flow in pure torsion is calculated using the torsional moment generated by the arm between the point of application of the aerodynamic loads (center of pressure) and the shear center. Finally, the pure shear and pure torsion flows are summed to find the total shear flow.

The shear flow in pure shear in each boom i is calculated according to Eq. (11).

$$\tau_{bi} = -\left(\frac{S_x I_{xx} + S_z I_{xz}}{I_{xx} I_{zz} - {I_{xz}}^2}\right) x_i B_i + \left(\frac{S_z I_{zz} + S_x I_{xz}}{I_{xx} I_{zz} - {I_{xz}}^2}\right) z_i B_i \tag{11}$$

where x_i and z_i are the boom i coordinates, S_X and S_Z are shear forces in the x and z directions, respectively, and I_{xx}, I_{zz} and I_{xz} are the moment of inertia in the x, z and xz directions, respectively. In this study, only the forces generated by the lift were estimated, therefore only the S_Z values are considered.

The shear flow in pure torsion in each boom i was calculated according to Eq. (12).

$$\tau_{b_i} = \frac{2A_i G_i \left(\frac{d\theta}{dy}\right)_i}{\oint_i \frac{ds}{t}} \tag{12}$$

where A_i is the area of each section's cell (region between spars), G_i is the shear modulus, t is the structural element thickness as a function of its length variation ds, and $d\theta$ is the torsion angle per d unit length induced by the torsional torque.

3. SIZING CRITERIA

3.1 Limit Stress Criterion

In possession of the components' normal and shear stresses, they can be compared with the limit stresses of their respective materials.

The allowable limit stress is defined verifying the minimum value between the yield limit σ_{yield} and ultimate limit σ_{ultimate} and their respective factor of safety FoS_{yield} and FoS_{ultimate} by the Eq. (13) relationship.

$$\sigma_{max} = min\left[\left(\frac{\sigma_{\text{yield}}}{FoS_{\text{yield}}}\right), \left(\frac{\sigma_{\text{ultimate}}}{FoS_{\text{ultimate}}}\right)\right] \tag{13}$$

As the structural elements are subjected to normal and shear stresses at the same time, the von Mises criterion for limit load is applied. This method is able to calculate a σ_{VM} stress equivalent to the stress tensor applied to each element. Equation 14 presents the von Mises criterion by considering the stresses in the Cartesian plane used in this study.

$$\sigma_{VM} = \sqrt{\frac{\left(\sigma_x - \sigma_y\right)^2 + \left(\sigma_y - \sigma_z\right)^2 + \left(\sigma_x - \sigma_z\right)^2 + 6\left({\tau_{xy}}^2 + {\tau_{yz}}^2 + {\tau_{xz}}^2\right)}{2}} \tag{14}$$

where σ are the normal stresses and τ the shear stresses. Their coefficients indicate the position in the Cartesian plane that the stresses are applied.

The von Mises criterion will be verified in all structural elements (spars, skin panels, stiffeners, and ribs). For better results quantification, Eq. (15) represents a margin of safety MS_{VM} which is defined by the ratio between the von Mises stress (σ_{VM}) and the specified limit stress (σ_{max}). In other words, the MS_{VM} value must be always greater than 0.

$$MS_{VM} = \frac{\sigma_{VM} - \sigma_{max}}{\sigma_{max}} > 0 \tag{15}$$

3.2 Stability Criteria

Stability criteria include failure conditions that can occur at stresses lower than the previously σ_{max} limit, caused by compressive and shear stresses in the form of buckling and crippling.

The methods used in this study to calculate instabilities in wing structures are those proposed by Gerard and Becker (1957). According to the literature, Eqs. (16) and (17) are used for calculating the critical stress in compression and shear loads, respectively. This method is used to evaluate the stability of panel elements (skin panels, spar webs and ribs).

$$\sigma_{C_{CR}} = \frac{\eta K_C \pi^2 E}{12\left(1 - \nu_e^2\right)}\left(\frac{t}{b}\right)^2 \tag{16}$$

$$\tau_{S_{CR}} = \frac{\eta K_S \pi^2 E}{12\left(1 - \nu_e^2\right)}\left(\frac{t}{b}\right)^2 \tag{17}$$

where t is the panel thickness, b is the panel length, E is the Young's modulus, ν_e is the Poisson's ratio, K_C is the buckling coefficient of plates subjected to compression stress, and K_S is the buckling coefficient of plates subjected to shear stress. The coefficients K_C and K_S are estimated using the abacuses provided in the literature of Gerard and Becker (1957), which consider the plates' geometry and boundary conditions. The factor η represents the plasticity correction factor, if the critical stresses found are in the plastic domain, this factor must be considered, being also estimated through abacuses

provided in the literature of Gerard and Becker (1957), which consider the yield strength and terms that represent the shape of the stress-strain curve of the material.

Equally, the margin of safety is evaluated for a better results understanding. In that case, it calculates the ratio between the critical stresses and the real applied stresses. If the value is less than 0, there is a condition of instability. In a wing design, the buckling is not tolerated, as this may lead to a local change in the aerodynamic profile, so the margin of safety must be always greater than the specified value. Equation 18 shows the margin of safety in a compression condition and Eq. (19) in a shear condition.

$$MS_C = \frac{\sigma_C - \sigma_{C_{CR}}}{\sigma_{C_{CR}}} > 0 \tag{18}$$

$$MS_S = \frac{\tau_S - \tau_{S_{CR}}}{\tau_{S_{CR}}} > 0 \tag{19}$$

The panels are also designed to work under combined compressive and shear loads, so the combined stress theory of Schildcrout and Stein (1949) can be applied by Eq. (20).

$$(MS_S + 1)^2 + (MS_C + 1) > 1 \tag{20}$$

For beam elements (stiffeners and spar caps) the Gerard and Becker (1957) literature proposes the calculation of the crippling critical stress, given by Eq. (21).

$$\sigma_{R_{CR}} = \alpha \sigma_{CY} \left[\left(\frac{t^2}{A} \right) \left(\frac{E}{\sigma_{CY}} \right)^{\frac{1}{3}} \right]^{\beta} \tag{21}$$

where t is the beam thickness, A is the beam cross-sectional area, E is the Young's modulus, and σ_{CY} is the yield stress of the material. The numerical factors α and β depend on the beam geometry.

In the same way as before, the crippling critical stress is compared with the actual load applied on the element, generating the margin of safety value, given by Eq. (22).

$$MS_R = \frac{\sigma_C - \sigma_{R_{CR}}}{\sigma_{R_{CR}}} > 0 \tag{22}$$

4. OPTIMIZATION ROUTINE

The theories presented up to this point are able to verify whether a structural element is capable or not to withstand the aerodynamic loads. Conversely, this analysis requires a predetermined architecture, where the components' thicknesses are known. To solve this issue, an optimization routine was implemented with the objective of finding a configuration that minimizes the wing final weight, estimating the optimum thickness for each structural element.

Under those circumstances, this work adopted the "differential evolution optimization algorithm" proposed in the literature of Storn and Price (1997). The differential evolution algorithm can be described as a stochastic meta-heuristic optimization method. The optimization is inspired by genetic algorithms and evolutionary strategies combined with a geometric research technique. Another key point is that genetic algorithms change the structure of individuals using mutation and crossing, while evolutionary strategies achieve self-adaptation through a geometric manipulation of individuals.

Initially, the user must provide the routine with basic project data, such as the flight conditions, overall geometrical dimensions of the wing and materials properties. Using these inputs, it is possible to estimate the lift coefficient and to calculate the shear forces and bending moments distribution with the methods presented in Section 2.1.

Only after these preliminary steps, the optimization algorithm is launched. In order to facilitate the convergence, the wing is divided into sections delimited by the ribs and the optimization is done individually for each section. The stresses in each section are calculated according to the methods in Sections 2.2, 2.3 and 2.4. The sizing criteria presented in Section 3 are evaluated and the margin of safety for each criterion can be verified. If all the margins are greater than the minimum allowed value, the weight of this section is calculated by the objective function. When one of the margins exceeds the minimum value, a penalty condition is applied. As the objective of the optimization algorithm is to minimize weight, the applied penalty is a very high value of weight ($9 \cdot 10^9$ kg), so this configuration is discarded by the optimization process.

The differential evolution algorithm uses the stop condition of the maximum number of generations. If at the end of the optimization the lowest weight found by the algorithm is generated by a penalty, an error message will appear asking the user to increase the maximum number of generations and/or to increase the thicknesses domain.

Once all the sections are designed, the wing total weight is calculated and the thicknesses values are presented to the user.

Figure 3 shows the optimization routine flowchart for each wing section.

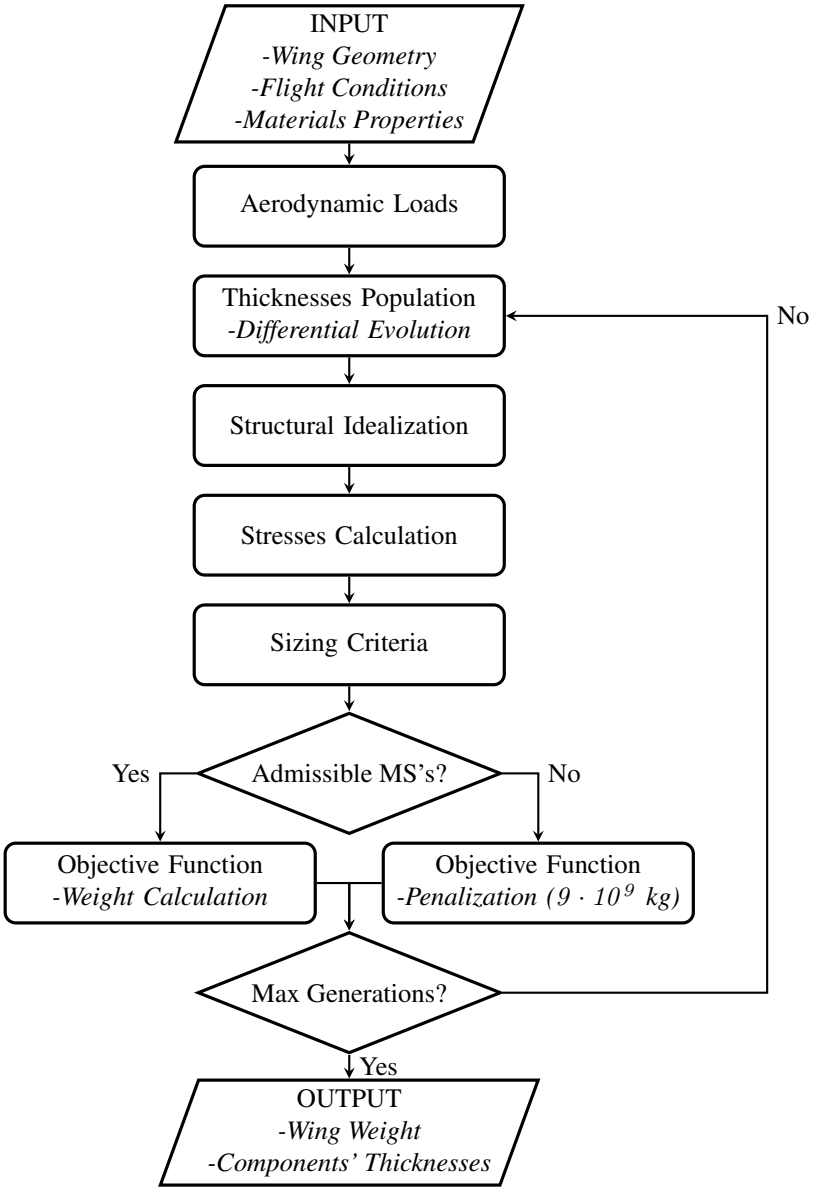

Figure 3. Optimization algorithm flowchart.

5. VALIDATION

The test case used to validate this study was the wing of the Dolphin 4000 hybrid-electric aircraft designed by Silva and Gil (2017). This aircraft was chosen because the authors had a direct participation in its development, ensuring that the data used for the validation are precise and reliable. Table 1 shows the input data used for the validation process.

Table 1. Parameters from the Dolphin 4000 hybrid-electric aircraft wing.

Domain	Characteristic	Value
Wing Geometry	Wingspan	13.38 m
	Root Chord	1.31 m
	Root Tip	0.92 m
	Airfoil	NACA 0012
Flight Conditions	Dynamic Pressure	2975.74 Pa
	Mach	0.29
	Max Load Factor	3.80
Materials Properties	Material	Al 7075-T6

5.1 Aerodynamic Loads

The aerodynamic load distribution validation was made comparing the analytical results obtained by the method proposed in Section 2.1 with simulations made through the software XFLR5 v6.47. This tool is capable of performing aerodynamic analyses on airfoils, wings, and planes operating at low Reynolds numbers. To do so, it is integrated with an interactive program for analysis of subsonic isolated airfoils called XFoil and then uses a panel method to calculate the three-dimensional lift distribution of a finite wing.

From the lift distribution, the shear forces and bending moments were obtained using the theory proposed by Eqs. (3) and (4). Figure 4 shows the lift distribution, shear force and bending moment distributions calculated by XFLR5 and the analytical method proposed in this work.

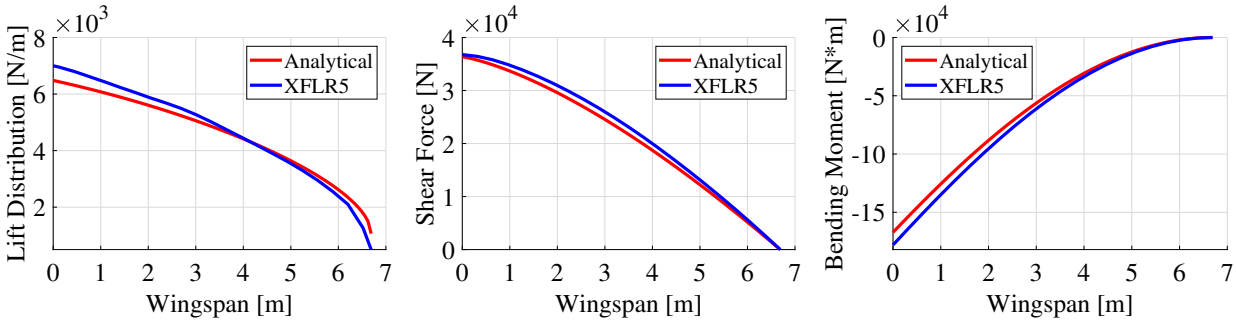

(a) Lift distribution (b) Shear force (c) Bending moment

Figure 4. Aerodynamic load along the wingspan calculated by XFLR5 and the analytical method proposed in this work.

The aerodynamic distributions shown in Fig. 4 ensure that the theories applied in this study produce results consistent with the XFLR5. Minor discrepancies in the distributions are possibly generated because the Schrenk (1941) distribution is based on approximations, while the software considers the actual wing geometry.

5.2 Optimization Algorithm

As presented in Section 4, the differential evolution algorithm has a stop condition as the maximum number of generations. In order to verify the correct convergence of the optimization process, the routine was launched five times varying its maximum number of generations. For this analysis, some optimization parameters were fixed in their default values proposed by Storn and Price (1997), such as the number of population individuals as 100, crossover probability as 0.5, and function stepsize factor as 0.8.

Moreover, the optimization process is done individually for each wing section (regions between ribs). The wing used in this study has 13 sections, in this way the optimization routine is launched 13 times using the same maximum number of generations. Figure 5a shows the mean wing weight values and its deviations for five launches within a domain of 50 to 500 generations, while Fig. 5b presents the associated calculation time.

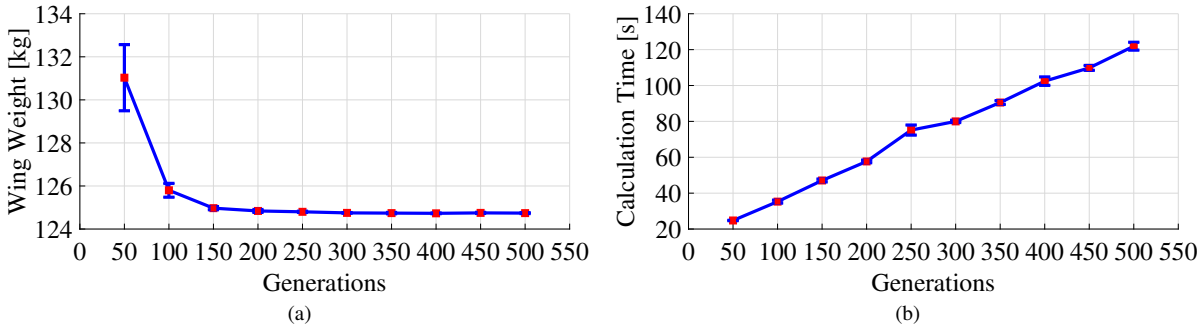

(a) (b)

Figure 5. Wing weight (a), calculation time (b) and their variations for five launches varying the maximum number of generations.

Through Fig. 5a it is possible to observe that after 300 generations the variations and mean values of weight become practically constant, however Fig. 5b shows that the calculation time grows linearly. In order to avoid calculations that are too long, the default value for the stop condition has been chosen as 300 generations.

Finally, the individual convergence of each wing section has been verified. For better data visualization, Fig. 6a shows the iterative process for the first six wing sections, while Fig. 6b shows for the last wing sections with a stop condition of 300 generations per section.

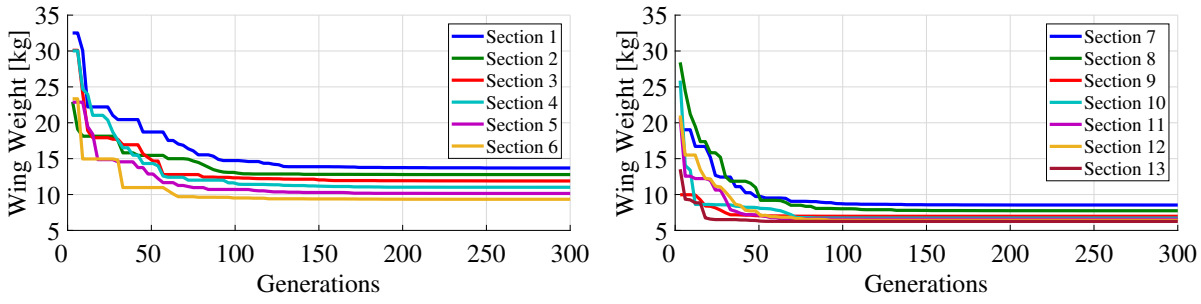

(a) (b)

Figure 6. Optimization process for the wing sections 1-6 (a) and sections 7-13 (b) with a stop condition of 300 generations per section.

5.3 Sizing

The sizing validation was performed comparing the results obtained by the proposed analytical-based optimization method with finite element method (FEM) simulations.

The Altair HyperMesh V13 software was used to generate the wing FE model. A total of 94 plate-shaped properties (PSHELL) were used to represent the skin panels, spar webs, and ribs thicknesses, while 52 beam-shape properties (PBEAML) represented the stiffeners and spar caps geometries. The final mesh size was 281,640 degrees of freedom.

Thereupon, the same thicknesses estimated by the analytical method were applied to the mesh properties and FEM simulations were performed using the MSC NASTRAN 2017 solver. The SOL 101 (Linear Static Analysis) and SOL 105 (Linear Buckling Analysis) were performed and their results were compared with the method proposed in this study.

Figure 7 shows a comparison between the von Mises stresses calculated by MSC NASTRAN SOL 101 and the analytical method, presented for each wing section.

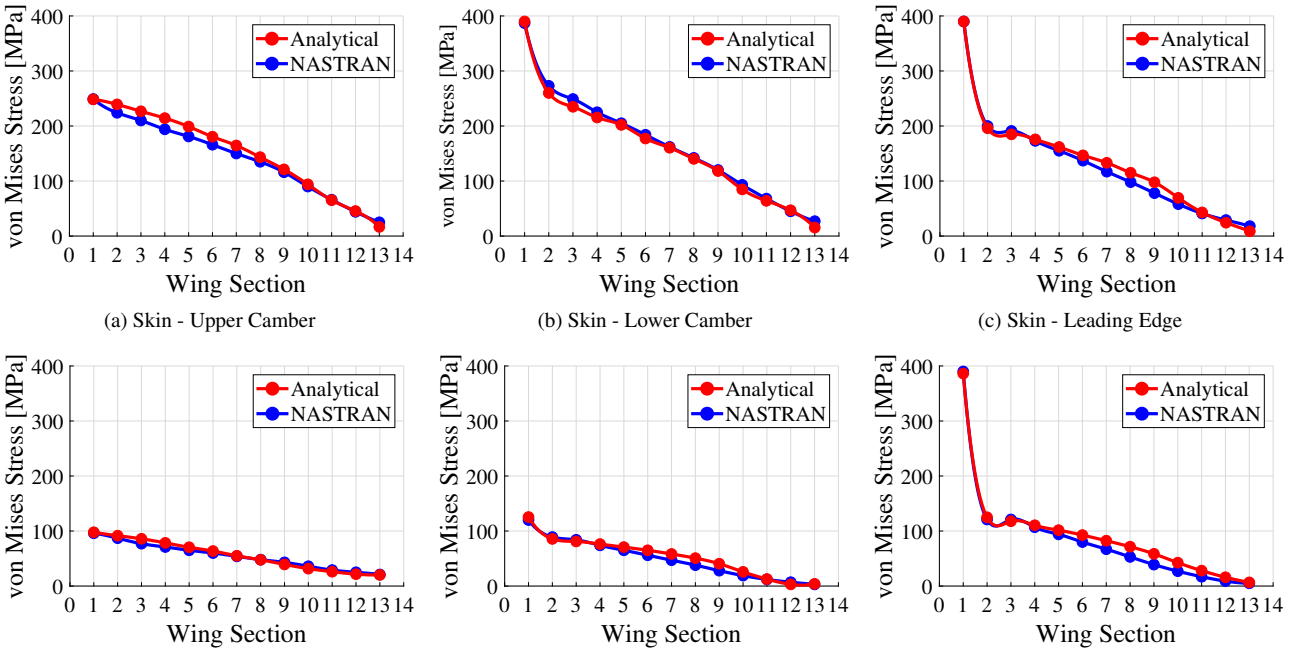

(a) Skin - Upper Camber (b) Skin - Lower Camber (c) Skin - Leading Edge

(d) Rib (e) Spar - Web (f) Spar - Cap

Figure 7. Von Mises stresses calculated by NASTRAN and the analytical method proposed in this work.

In addition, the first buckling mode estimated by MSC NASTRAN SOL 105 indicated an eigenvalue of 1.013, while the analytical method estimated that value at 1.000.

Additionally, with the same FE mesh, the MSC NASTRAN 2017 SOL 200 (Design Sensitivity and Optimization Analysis) was launched as a way to compare the weight and thicknesses found by the analytical-based optimization method with a second and different optimization logic.

The MSC NASTRAN 2017 SOL 200 is a multidisciplinary gradient-based optimization which searches discrete solutions within a design space around a continuous optimum. The optimization variables were the thicknesses from the

FE mesh properties (PSHELL and PBEAML) and the objective was to minimize the wing weight. Moreover, the same constraints used on the analytical-based optimization were applied to the SOL 200, namely: maximum von Mises stress of 390 MPa, first buckling eigenvalue of 1 and minimum thickness of 1.6 mm.

Given these points, MSC NASTRAN 2017 SOL 200 performed an optimization with 146 optimization variables using the previously described FE mesh. The solution converged to an optimum point after 18 design cycles. Figure 8 shows a comparison between the thicknesses found by the MSC NASTRAN 2017 SOL 200 and those found by the analytical-based optimization, presented for each wing section.

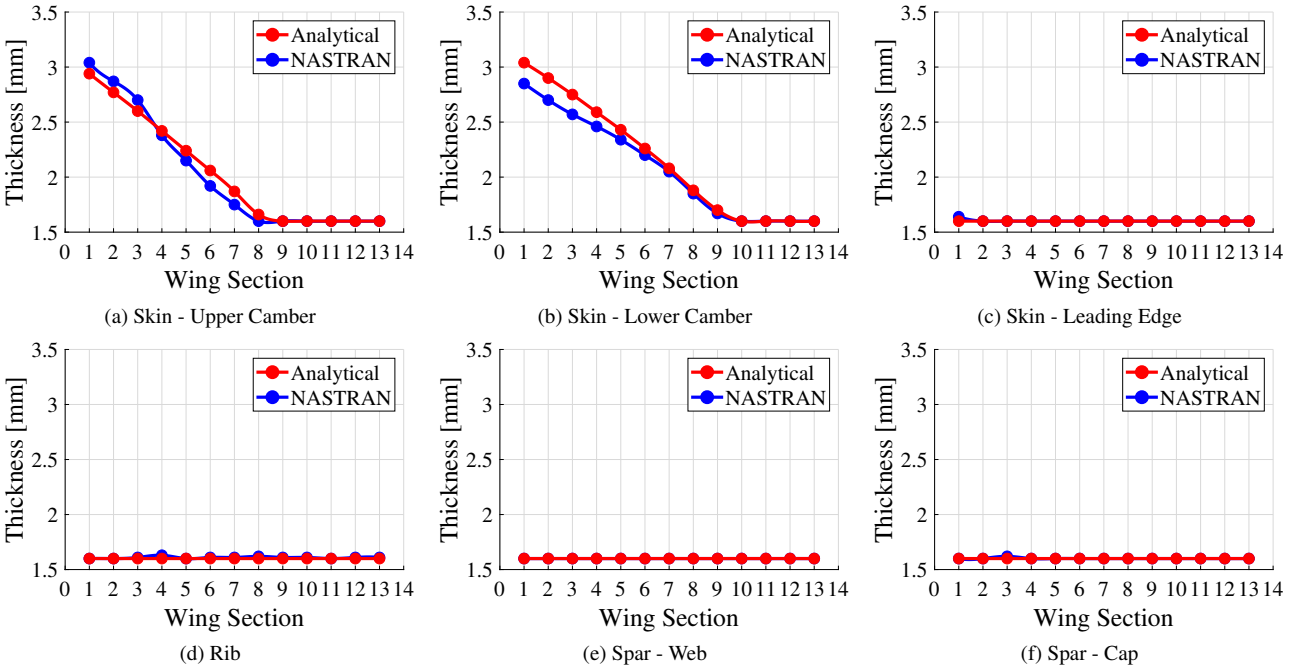

(a) Skin - Upper Camber (b) Skin - Lower Camber (c) Skin - Leading Edge

(d) Rib (e) Spar - Web (f) Spar - Cap

Figure 8. Thicknesses optimized by NASTRAN and the analytical method proposed in this work.

The data from Fig. 8 show that the calculated thicknesses in both optimizations are consistent. Only a few divergences were found in the skin panels region (Figs. 8a and 8b). Their possible causes will be further discussed in Section 6.

Furthermore, Tab. 2 presents the weight estimated by the two optimization methods and their calculation time.

Table 2. Wing weight and calculation time of the analytical-based optimization and MSC NASTRAN 2017 SOL 200.

Parameter	Analytical-Based Optimization	MSC NASTRAN 2017 SOL 200
Wing Weight	124.75 kg	119.73 kg
Calculation Time	00:01:20	00:39:33

In comparison, it was verified what weight statistical methods would estimate for this wing. Hence, the methodology proposed by Raymer (2018) was used, which considers wing geometric factors and mission data in its formulation. The calculated value for this wing weight was 101.78 kg, which is well below the values predicted by the analytical-based optimization and the MSC NASTRAN 2017 SOL 200.

6. DISCUSSION

The results discussed in Section 5 showed that the theories used for this study are consistent with their validation methods, especially for aerodynamic loads and internal stresses calculation. The only notable difference is the thickness estimation and consequently the wing final weight obtained through the MSC NASTRAN 2017 SOL 200. Some possible causes of these discrepancies can be discussed.

First, as stated by Megson (2016), the structure idealization method sacrifices the calculation precision for a higher calculation speed. Due to the loss of information during the idealization process, the equivalent structure must be more robust than the original in order to avoid any under conservatism.

Second, the analytical optimization process is performed individually for each wing section, generating some simplifications. For instance, the support conditions between the sections are considered as ideal by the analytical method, reflecting at the buckling coefficients found in the literature abacuses, while the FEM simulation can generate more re-

alistic boundary conditions. Under those lines, the FEM optimization considers the wing as a whole, generating a better distribution of internal forces. In this way, the stiffness of a given section can influence its neighboring regions, helping to decrease the wing final weight.

Moreover, the weight difference in relation to the statistical method can be explained through its own origin. Statistical formulations are generated through real data obtained from commercial aircraft. However, this wing design escapes the standard trend, both in its eccentric application (hybrid-electric aircraft) as in its unusual geometric proportions (aspect ratio of 12.8).

After all, for this test case, the objective of this work was reached. The analytical-based method was able to generate a more accurate result when compared to statistical methods, requiring a lower computational cost when compared to a more sophisticated optimization. Nonetheless, the results should be interpreted with caution and a number of limitations must be borne in mind.

The analytical approach does not consider any type of elastic deformation. This approach can directly affect the aerodynamic loads estimation and internal stresses calculations. In addition, aeroelastic phenomena such as divergence and flutter are not considered in the sizing criteria, being factors that can directly influence the wing final weight.

Moreover, this method does not consider any type of deflection of movable parts that can generate additional aerodynamic loads. Therefore, its use for an empennage design can generate unreliable results.

Also, the theories consider only isotropic materials, in special aeronautical aluminum alloys. Consequently, wing designs in composite material can not be performed by the method presented in this study.

After acknowledging the method limitations, future works may be proposed in order to overcome the above limitations. One way to accomplish this would be to apply new theories that would consider the limiting points of the project. In addition, it would be interesting to test further cases, in order to have a deeper knowledge about the sizing reliability.

7. CONCLUSION

To sum up, the theories used in the analytical-based optimization approach were satisfactorily validated, showing that this method is capable of generating accurate results.

Likewise, when compared to a more accurate optimization routine, the analytical method presented a conservative difference in the final weight of 4.11% and was able to perform the calculation approximately 30 times faster. In addition, the analytical approach proved to be more reliable than statistical methods, which estimated a weight 16.21% lower than expected.

In conclusion, the objective of this work was reached, where it was expected to create an analytical method capable of designing a wing faster than the traditional computational simulations, but with high-reliability results.

8. REFERENCES

Bonnet, A. and Luneau, J., 1989. "Aerodynamique: theories de la dynamique des fluides". *Cepadues Editions, Toulouse*.

de Weck, O., Agte, J., Sobieszczanski-Sobieski, J., Arendsen, P., Morris, A. and Spieck, M., 2007. "State-of-the-art and future trends in multidisciplinary design optimization". In *48th AIAA/ASME/ASCE/AHS/ASC Structures, Structural Dynamics, and Materials Conference*. p. 1905.

Gerard, G. and Becker, H., 1957. *Handbook of Structural Stability: Parts I-VI*. NACA - National Advisory Committee for Aeronautics.

McMasters, J.H. and Cummings, R.M., 2002. "Airplane design-past, present, and future". *Journal of Aircraft*, Vol. 39, No. 1, pp. 10–17.

Megson, T.H.G., 2016. *Aircraft structures for engineering students*. Butterworth-Heinemann.

Murman, E.M. and Rizzi, A., 2002. "Integration of CFD into aerodynamics education". In *Frontiers Of Computational Fluid Dynamics 2002*, World Scientific, pp. 493–506.

Raymer, D., 2018. *Aircraft design: a conceptual approach*. American Institute of Aeronautics and Astronautics, Inc.

Rivello, R.M., 1969. *Theory and analysis of flight structures*. McGraw-Hill College.

Schildcrout, M. and Stein, M., 1949. "Critical combinations of shear and direct axial stress for curved rectangular panels".

Schrenk, O., 1941. "A simple approximation method for obtaining the spanwise lift distribution". *The Aeronautical Journal*, Vol. 45, No. 370, pp. 331–336.

Silva, H.L. and Gil, A.A., 2017. "Hybrid-electric aircraft: conceptual design, structural and aeroelastic analyses".

Storn, R. and Price, K., 1997. "Differential evolution–a simple and efficient heuristic for global optimization over continuous spaces". *Journal of global optimization*, Vol. 11, No. 4, pp. 341–359.

Torenbeek, E., 2013. *Advanced aircraft design: conceptual design, analysis and optimization of subsonic civil airplanes*. John Wiley & Sons.

9. RESPONSIBILITY NOTICE

The authors are the only responsible for the printed material included in this paper.